

# THE DIVERGING SPHERE AND THE RIB IN PROMPT DETONATION

P. Clark Souers, Estella McGuire, Raul Garza, Frank Roeske and Peter Vitello  
Energetic Materials Center  
Lawrence Livermore National Laboratory,  
Livermore, California, 94550, USA

Steady state corner-turning in a  $90^\circ$  rib (or arc) is possible if  $R_0/R_1 \ll 0.15$ , where  $R_0$  is the half-width and  $R_1$  the inner radius. For thicker ribs, the explosive kinetics will further slow the turn. A steady state turn will not have a symmetrical detonation front but will bow inward. A very tight tight turn experimentally shows signs of turbulence. The inverse-radius relation appears to approximately hold for the diverging sphere, at least for large radii. The reaction zone lengths for diverging spheres and ratesticks increase with the radius of curvature and are comparable. The sphere is sensitive to the means of initiation and it is difficult to tell if steady state has been achieved.

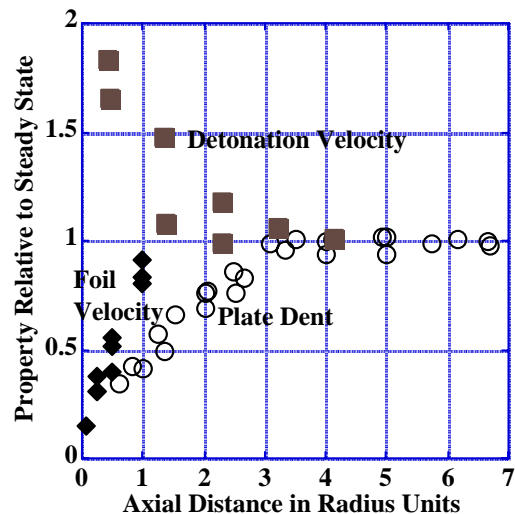
## CYLINDRICAL GEOMETRY

Before moving to unusual geometries, we consider cylindrical symmetry, where most data has been taken. The distance to steady state conditions is important as shown in Figure 1 for bare cylinders (ratesticks). The diamonds are PBX 9502 reaction zone lengths obtained from Visar traces reflected from a metal foil on the explosive with a transparent “impedance-matching” material in front.<sup>1</sup> The distance from the spike to the C-J point is a measure of the reaction zone length.<sup>2</sup> A Comp B booster with an aluminum smoothing plate was used. The squares are 1.62 g/cc TNT pressed at  $65^\circ\text{C}$  and boosted with PBX 9205 for which plate dent depths are measured.<sup>3</sup> This depth is generally considered to be a measure of the total detonation energy. The circles and triangles are the detonation velocity for AN 80%-TNT boosted by different amounts of RDX. The AN/TNT is overdriven by different amounts and the detonation velocity eventually finds steady state.<sup>4</sup>

The x-axis in Figure 1 is plotted in units of the ratestick radius. For about one and a third radius units, the measurement, taken on the axis, is unaware of the edge of the ratestick. Then the rarefaction wave arrives and oscillates sideways in the explosive for at least 4–5 radial distances until steady state is achieved. This steady state is caused by energy loss from the sides of the ratestick.

The plate dent data increased linearly as the radius was increased from 6 to 20 mm. It seems

likely, however, that eventually the energy delivered into the dent will become constant. The reaction zone length increases in Figure 1 as the 0.63 power of the radius, but some evidence suggests that, at a large radius, the detonation front curvature becomes so flat that individual grains can break up the reaction zone.<sup>5</sup> This could bring the reaction zone length to some saturation value at large radii. The point is that no search for an internally-created steady state condition has yet been made.





$$t_2 \approx \frac{2R_o}{3U_s} = \frac{8R_o}{4 \cdot 3U_s} \quad (5)$$

where the sound speed is taken as 3/4ths the detonation velocity. The time to move along the inner edge to the measuring angle is given by

$$t_1 = \frac{X}{360} \frac{2\pi R_1}{U_s} \quad (6)$$

In order to reach energy equilibration, we need about 4 reverberations of the energy across the rib, which is 4 rate time constants or

$$4(t_2 + t) < t_1 \quad (7)$$

For an ideal explosive, with  $t \approx 0$ , we expect equilibration at

$$\frac{R_o}{R_1} < 1.64e - 3\psi, \quad (8)$$

which gives 0.15 for  $\psi = 90^\circ$ . Only thin ribs can reach steady state.

In the turn,  $U_{ss}$  continues to represent a physical velocity as the detonation moves along the inner edge. However, the detonation pushes across the explosive front to the outer edge. The wave velocity measured by moving around the outer edge,  $W \gg U_s$ , will not be physical but simply represent when the short-cutting front arrived there. The front may be said to have equilibrated if  $U_{ss}$  and  $W$  approach a constant. It will have reached a rigid body condition if the velocities are proportional to the radii:

$$\frac{U_{ss}}{W} = \frac{R_1}{R_1 + 2R_o} \quad (9)$$

Eq. 9 is important because  $W$  is experimentally easier to measure than  $U_{ss}$  and may be used to obtain  $U_{ss}$ .

From Eq. 9, we get that

$$\frac{U_{ss}}{U_s} = \frac{R_1}{R_1 + R_o} \quad (10)$$

which illustrates the relation of the original straight section detonation velocity, which had

the leading point in the center. We may rewrite Eq. 10 as

$$1 - \frac{U_{ss}}{U_s} = \frac{R_o}{R_1 + R_o} \quad (11)$$

We consider a radius drawn to the leading point of the detonation front as it turns (OBD in Figure 2). This point would occur on the inner edge for an ideal explosive, but it occurs a distance  $\Delta R$  in from the inner edge for a real explosive. The lag along the inner edge,  $L_o$ , is small but is related to the reaction rate. The lag on the outer edge,  $L_1$ , is large and occurs because of the time it takes for the outside-edge wave velocity to increase from  $U_s$  to  $W$ . If this velocity were  $U_s$  for one time constant of Eq.6, then switched to  $W$ , we would have an angle  $\Theta$  of  $\tan^{-1}(4/3) = 53^\circ$ . If steady state is achieved, then this lag will be constant; otherwise, it will continue to grow with increasing  $\psi$ .

Not much rib data exists, and we will use code runs using JWL++, a simple reactive flow model in a 2-D ALE (arbitrary Lagrangian-Eulerian) code, which runs mainly in the Lagrange mode.<sup>8,12,13</sup> All runs are at the edge of convergence, which means there are at least 4 zones in the reaction zone for the smallest size part. The nearest-ideal explosives run are Comp B, LX-17 and RX-08-HD, all with the reaction time constant of about 0.02  $\mu s$ . Non-ideal explosives include PBXN-111 (0.4  $\mu s$ ), amatol (0.7  $\mu s$ ) and dynamite (1  $\mu s$ ).

Figure 3 shows inner (lower one in each pair) and outer-edge wave velocities for two calculated dynamite ribs. The lower pair has come to steady state in the turn and the velocities are constant. The outer-edge velocity overshoot and is decreasing slightly. The overall velocities are low because a narrow rib is needed to achieve steady state, and the size (diameter) effect is at work. The upper pair with a broad width never reaches steady state and the outer-edge wave velocity is still increasing. Using a long straightaway section to ensure steady state at the start is important to quickly achieving steady state in the turn. From Eq. 9, we obtain  $((W/U_{ss})(1 + 2R_o/R_1))$ , where  $W$  and  $U_{ss}$  are the values taken as close to a 90°-turn as possible. We find that this ratio is always near 1, even though the detonation velocities themselves have not fully equilibrated.

We next calculate the near-90° inner-edge detonation velocities for various ribs of dynamite, and these are seen in Figure 4. Some points are at steady state and some are not. An inverse radius ( $1/R_0$ ) plot similar to that of the size (diameter) effect is used. The topmost curve is that of straight slabs. As  $R_1$  decreases, the detonation velocity also decreases. At some point, the inner radius becomes so tight that failure must occur in real explosives.

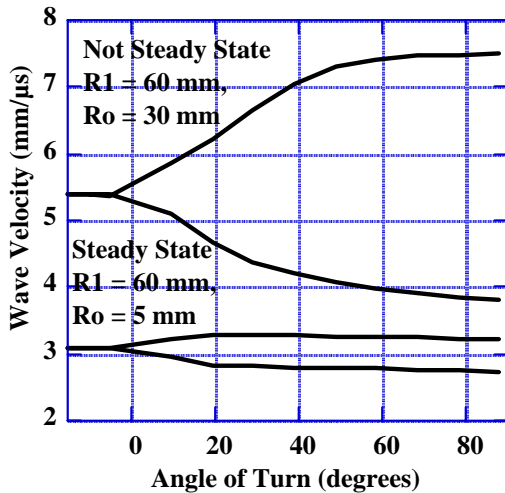


FIGURE 3. WAVE VELOCITY CURVES CHANGE SHAPE WITH SIZE.

We turn to prediction of the inner edge detonation velocity. Normalized results are shown in Figure 5 with the open symbols being code runs and the closed symbols being LX-17 data. The Y-axis is  $U_{ss}/U_s - 1$ , the fractional decrease in the inner edge velocity. We make it negative so the width goes from thin to fat as we go left to right. The top curve contains the near-ideal explosives and the bottom curve the non-ideal explosives. We see that all the points fall on the same line for  $R_0/R_1 < 0.15$ , ie in the region of energy equilibration. For  $R_0/R_1 > 0.15$ , the ribs never equilibrate by 90° and kinetic effects are important. The slower the detonation rate, the lower will be the inner edge velocity. The JWL++ model says that geometry is the cause of inner-edge effects.

Figure 6 shows calculated detonation front curvatures for RX-08-HD with  $R_1 = 10$  mm and  $R_0 = 1.5$  mm with a 9 mm thick Lucite case. The

top horizontal line is the radius drawn through the leading point of the front. The lags are downward, so that the detonation is proceeding upward. The model does not get the curvature right-  $\Delta R$  is larger for the measured value. But the important thing is that the leading edge is closer to the inner than the outer edge. This is true even at steady state- the detonation front is no longer symmetric as it was in the straightaway.

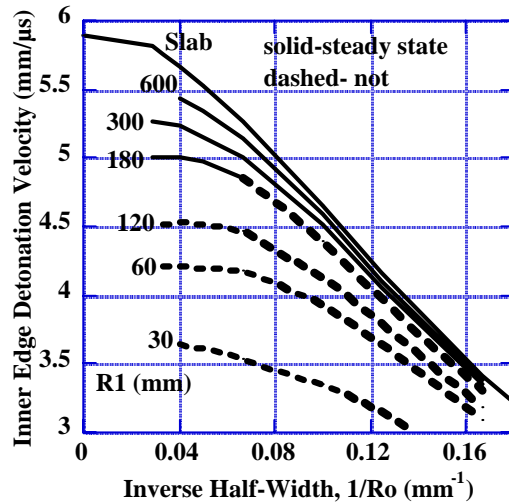


FIGURE 4. "SIZE-EFFECT"-TYPE CURVES FOR DYNAMITE RIBS.

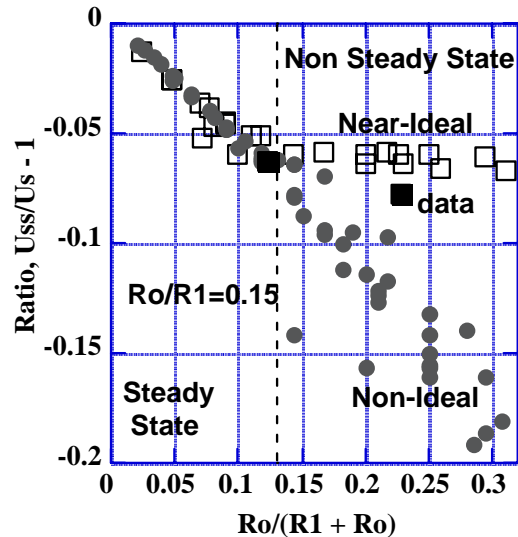
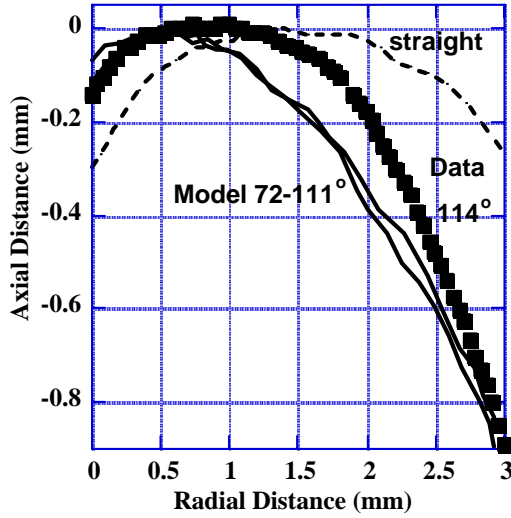
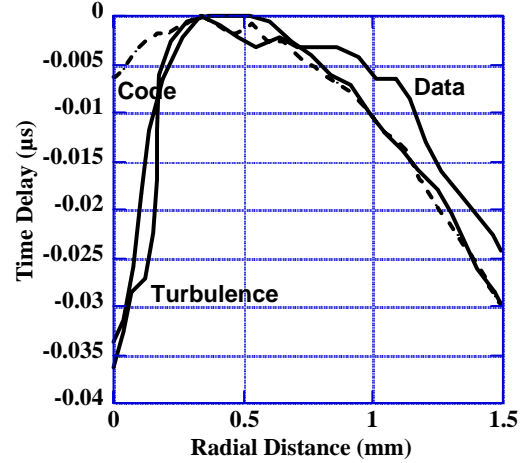


FIGURE 5. THE INNER EDGE VELOCITY DECREASES WITH THE INCREASING RIB WIDTH.

Extremely wide ribs are interesting. Figure 7 shows the inner half of RX-08-HD detonation fronts measured for two 3 mm copper-clad samples with a right angle turn only 2.5 mm after the start of the turn.<sup>11</sup> The data, shown by the solid lines, is far from steady state. The dashed line is the calculated front. Extra code runs are needed to obtain the velocity at each point so that a conversion from a distance plot to a time plot may be made. The measured inner edge lag,  $L_o$ , is larger than expected and appears turbulent on the inner edge. The model is not capable of showing this kind of behavior.



**FIGURE 6. DETONATION FRONT CURVATURES FOR RX-08-HD WITH  $R_1 = 10$  MM,  $R_0 = 1.5$  MM.**



**FIGURE 7. TURBULENT DETONATION FRONTS SEEN IN RIGHT ANGLE TURNS.**

### THE DIVERGING SPHERE

This problem never sees an external wall and so must contain an internal kind of equilibrium state different from the edge process. What makes this problem so difficult is 1) we can never set a true steady state initial condition, and 2) real detonators may deviate from this equilibrium and we will not know. The true equilibrium was postulated by Eyring, et al. to vary as the well-known inverse radius.<sup>6</sup> We consider a simple approach with a spherical slice of volume  $4\pi/3[R^3 - (R - \langle x_e \rangle / 2)^3]$ , which produces a detonation energy, part of which is pushed forward to compress the next slice of undetonated explosive with the compression energy,  $E_c$ . We also make the assumption used in the ratestick derivation that the compression energy is proportional to the square of the detonation velocity. In a diverging sphere, the next slice to be compressed is larger than the one supplying the energy, so we have

$$\frac{E_c(\text{next})}{E_c} = \frac{R^3 - (R - \langle x_e \rangle / 2)^3}{(R + \langle x_e \rangle / 2)^3 - R^3} = \left( \frac{U_s}{D} \right)^2 \quad (12)$$

We expand the two cubic terms, divide one by the other and take approximations for  $\langle x_e \rangle / R \ll 1$ . The result is

$$\frac{U_s}{D} = \left(1 - \frac{3 \langle x_e \rangle}{R}\right)^{1/2} \approx 1 - \frac{3 \langle x_e \rangle}{2R} \quad (13)$$

We may say that the Eyring relation is probably a useful approximation that holds for the diverging sphere only for large radius.

Thus does the curvature of the detonation front control the velocity of the chemical reaction. This is the underlying principal of the DSD<sup>9</sup> and WBL<sup>14</sup> models for cylinders, but in the sphere, its effect will be stronger. Eq. 13 looks like the Eyring equation (Eq. 1) for large radius, but the constant here is the reaction zone length itself. The detonation front curvature is set completely by the geometry and there is no edge lag.

Figure 8 shows diverging sphere detonation velocity data plotted as detonation velocity versus inverse radius (negative to make larger radii to the right). The hemisphere data of Bahl, Lee and Weingart is for LX-17 (92.5% TATB/Kel-F, density 1.90 g/cc and the data of Aveille et al is for T2 (97% TATB, binder not named, density 1.855 g/cc)<sup>15,16</sup> The data

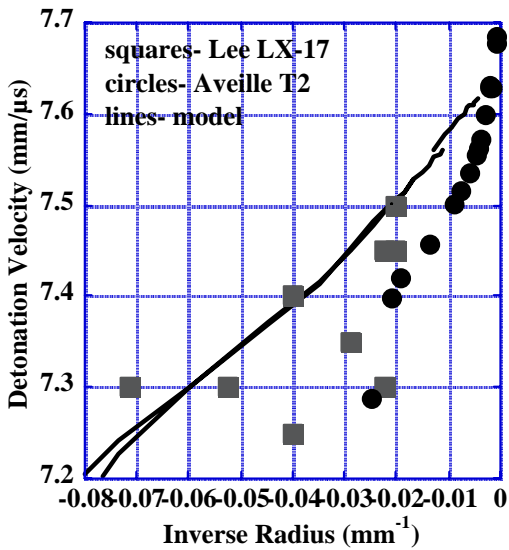


FIGURE 8. INVERSE RADIUS PLOTS FOR DIVERGING SPHERICAL TATB.

itself only roughly follows a straight line.

The lines are code runs, which are extremely sensitive to the initiation. An initiation of low power either fails or struggles to rise up

to the expected velocities. Once up, the curves are largely independent of the booster. (7)

We next compare reaction zone lengths from different sources. In a cylinder, the edge angle  $\alpha$  is defined as the angle between the normal to the front at the edge at radius  $R_0$  and the axis direction. The front is not circular but is a mixture of quadratic and a steeper edge effect. To compare with sphere data, we take as the radius of curvature the value at the edge where the reaction zone is defined by the edge lag. We have

$$R_{cur} = \frac{R_0}{\cos \alpha} \quad (14)$$

For the sphere, the radius of  $R$  is known and the reaction zone comes from the right side of Eq. 13. The detonation front curvature data for TATB ratesticks and a few copper-clad cylinders consists of LX-17, PBX 9502 (95% TATB/Kel-F) and T2.<sup>17-20</sup> High-HMX ratesticks include LX-10, LX-14 (95.5% HMX/estane), PBX 9404 (HMX 94%), PBX 9501 (HMX 95%), and X1.<sup>17,21,22</sup> The hemispheres include LX-17 and LX-10,<sup>15</sup> and the French logospheres are T2 and X1.<sup>22</sup> Figure 9 shows that the reaction zone lengths increase with increasing radius of curvature, and given the assumptions, the ratestick and sphere data are in agreement. The reaction zone length increases with the radius of curvature, ie inversely to the curvature.

We can define the detonation rate from Eq. 2 to be

$$v_f = \frac{2U_s D}{3[\langle x_e \rangle + \frac{1}{R} \frac{\partial \langle x_e \rangle}{\partial (1/R_0)}]} \quad (15)$$

Because the reaction zone length increases with radius, so does the detonation rate.

## CONCLUSIONS

After the cylinder, the rib and the sphere are the simplest geometries for basic analysis. Like a cylinder, the rib may be brought to a steady state independent of the initiation, but only for thin specimens. The diverging sphere is probably never detached from the means of initiation, and

the predicted steady state behavior is likely an approximation.

## ACKNOWLEDGEMENTS

We would like to thank Ron Lee for his continued interest in the sphere. This work was performed under the auspices of the U.S. Department of Energy by the University of California, Lawrence Livermore National Laboratory under Contract No. W-7405-Eng-48.

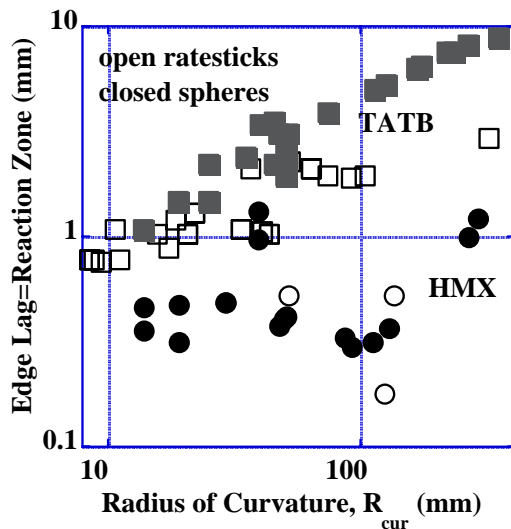


**FIGURE 9. REACTION ZONE LENGTHS INCREASE WITH THE RADIUS OF CURVATURE.**

## REFERENCES

1. W. L. Seitz, H. L. Stacy, Ray Engleke, P. K. Tang and J. Wackerle, "Detonation Reaction-Zone Structure of PBX 9502," Proceedings Ninth Symposium (International) on Detonation, Portland, OR, August 28-September 1, 1989, 657-669.
2. P. Clark Souers, "Measuring Explosive Non-Ideality," 1999 International Workshop on the Modeling of Non-Ideal Explosives," New Mexico Tech, Socorro, NM, March 16-18, 1999, proceedings.
3. LASL Explosive Property Data, T. R. Gibbs and A. Popolato (University of California, Berkeley, 1980).
4. S. Cudzilo, A. Maranda, J. Nowaczewski and W. Trzcinski, "Shock Initiation Studies of Ammonium Nitrate Explosives," *Comb & Flame* 102, 64-72 (1995).
5. P. C. Souers and Raul Garza, "Size Effect and Detonation Front Curvature," 1997 American Physical Society, Topical Group on Shock Compression of Condensed Matter, Amherst, MA, July 28-August 1, 1997, pp. 325-328.
6. H. Eyring, R. E. Powell, G. H. Duffey and R. B. Parlin, "The Stability of Detonation," *Chem. Rev.* 45, 69-181 (1949).
7. P. Clark Souers and Raul Garza, "Kinetic Information from Detonation Front Curvature." Eleventh International Detonation Symposium, Snowmass Village, CO, August 30-September 4, 1998, pp. 459-465.
8. P. Clark Souers, Steve Anderson, Estella McGuire, Michael J. Murphy, and Peter Vitello, "Reactive Flow and the Size Effect," *Propellants, Explosives, Pyrotechnics*, 26, 26-32 (2001).
9. J. D. Bdzil, W. Fickett and D. S. Stewart, "Detonation Shock Dynamics: A New Approach to Modeling Multi-Dimensional Detonation Waves," in Proceedings Ninth Symposium (International) on Detonation, Portland, OR, August 28-September 1, 1989, vol. II, pp. 730-742.
10. P. C. Souers, S. R. Anderson, B. Hayes, J. Lyle, E. L. Lee, S. M. McGuire and C. M. Tarver, "Corner Turning Rib Tests on LX-17," *Propellants, Explosives, Pyrotechnics*, 23, 1-8 (1998).
11. Frank Roeske and P. Clark Souers, "Corner Turning of Detonation Waves in an HMX-Based Explosive," *Propellants, Explosives, Pyrotechnics*, 25, 1-7 (2000).
12. P. Clark Souers, Steve Anderson, Estella McGuire and Peter Vitello, "JWL++: A Simple Reactive Flow Code Package for Detonation," *Propellants, Explosives, Pyrotechnics*, 25, 54-58 (2000).
13. P. Clark Souers, Jerry W. Forbes, Laurence E. Fried, W. Michael Howard, Steve Anderson,

Shawn Dawson, Peter Vitello and Raul Garza, "Detonation Energies from the Cylinder Test and CHEETAH V3.0," *Propellants, Explosives, Pyrotechnics* 26, 180-190 (2001).

14. B. D. Lambourn and D. C. Swift, "Applications of Whitham's Shock Dynamics Theory to the Propagation of Divergent Detonation Waves," *Proceedings Ninth Symposium (International) on Detonation*, Portland, OR, August 28- September 1, 1989, pp. 7840-797.

15. K. L. Bahl, R. S. Lee and R. C. Weingart, "Velocity of Spherically-Diverging Detonation Waves in RX-26-AF, LX-17 and LX-10," *Shock Waves in Condensed Matter- 1983*, J. R. Asay, R. A. Graham and G. K. Smith, eds., Elsevier Science Publishers, pp. 559-562 (1984).

16. J. Aveille, J. Baconin, N. Carion and J. Zoe, "Experimental Study of Spherically Diverging Detonation Waves," *Proceedings Eighth Symposium (International) on Detonation*, Albuquerque, NM, July 15-19, 1985, pp. 151-156.

17. LLNL Cylinder Test library, P. C. Souers, Lawrence Livermore National Laboratory, Livermore, CA.

18. John Bdzil, Los Alamos National Laboratory, Los Alamos, NM, private communication, 1996

19. L. G. Hill, J. D. Bdzil and T. D. Aslam, "Front Curvature Rate Stick Measurements and Calibration of the Detonation Shock Dynamics Model for PBX 9502 over a Wide Temperature Range," *Eleventh International Detonation Symposium*, Snowmass Village, CO, August 31-September 4, 1999.

20. F. Chaisse' and J. N. Oeconomos, "The Shape Analysis of a Steady Detonation Front in Right Circular Cylinders of High Density Explosive. Some Theoretical and Numerical Aspects," *Proceedings Tenth Symposium (International) on Detonation*, Boston, MA, July 12-16, 1993, pp. 50-57.

21. J. B. Bdzil, *J. Fluid Mech.* 108, 195-226 (1981).

22. F. Chaisse, J. M. Servas, J. Aveille, J. Baconin, N. Carion and P. Bongrain, "A Theoretical Analysis of the Shape of a Steady Axisymmetrical Reactive Shock Front in Cylindrical Charges of High Explosive, A Curvature-Diameter Relationship," *Proceedings Eighth Symposium (International) on Detonation*, Albuquerque, NM, July 15-19, 1985, pp. 159-167.